

Search for the rare decay $W^\pm \rightarrow \pi^\pm + \gamma$ in proton-antiproton collisions at $\sqrt{s} = 1.8$ TeV

- F. Abe,¹⁷ H. Akimoto,³⁹ A. Akopian,³¹ M. G. Albrow,⁷ A. Amadon,⁵ S. R. Amendolia,²⁷ D. Amidei,²⁰ J. Antos,³³ S. Aota,³⁷ G. Apollinari,³¹ T. Arisawa,³⁹ T. Asakawa,³⁷ W. Ashmanskas,¹⁸ M. Atac,⁷ P. Azzi-Bacchetta,²⁵ N. Bacchetta,²⁵ S. Bagdasarov,³¹ M. W. Bailey,²² P. de Barbaro,³⁰ A. Barbaro-Galtieri,¹⁸ V. E. Barnes,²⁹ B. A. Barnett,¹⁵ M. Barone,⁹ G. Bauer,¹⁹ T. Baumann,¹¹ F. Bedeschi,²⁷ S. Behrends,³ S. Belforte,²⁷ G. Bellettini,²⁷ J. Bellinger,⁴⁰ D. Benjamin,³⁵ J. Bensinger,³ A. Beretvas,⁷ J. P. Berge,⁷ J. Berryhill,⁵ S. Bertolucci,⁹ S. Bettelli,²⁷ B. Bevensee,²⁶ A. Bhatti,³¹ K. Biery,⁷ C. Bigongiari,²⁷ M. Binkley,⁷ D. Bisello,²⁵ R. E. Blair,¹ C. Blocker,³ S. Blusk,³⁰ A. Bodek,³⁰ W. Bokhari,²⁶ G. Bolla,²⁹ Y. Bonushkin,⁴ D. Bortoletto,²⁹ J. Boudreau,²⁸ L. Breccia,² C. Bromberg,²¹ N. Bruner,²² R. Brunetti,² E. Buckley-Geer,⁷ H. S. Budd,³⁰ K. Burkett,²⁰ G. Busetto,²⁵ A. Byon-Wagner,⁷ K. L. Byrum,¹ M. Campbell,²⁰ A. Caner,²⁷ W. Carithers,¹⁸ D. Carlsmith,⁴⁰ J. Cassada,³⁰ A. Castro,²⁵ D. Cauz,³⁶ A. Cerri,²⁷ P. S. Chang,³³ P. T. Chang,³³ H. Y. Chao,³³ J. Chapman,²⁰ M.-T. Cheng,³³ M. Chertok,³⁴ G. Chiarelli,²⁷ C. N. Chiou,³³ F. Chlebana,⁷ L. Christofek,¹³ M. L. Chu,³³ S. Cihangir,⁷ A. G. Clark,¹⁰ M. Cobal,²⁷ E. Cocco,²⁷ M. Contreras,⁵ J. Conway,³² J. Cooper,⁷ M. Cordelli,⁹ D. Costanzo,²⁷ C. Couyoumtzelis,¹⁰ D. Cronin-Hennessy,⁶ R. Culbertson,⁵ D. Dagenhart,³⁸ T. Daniels,¹⁹ F. De Jongh,⁷ S. Dell'Agnello,⁹ M. Dell'Orso,²⁷ R. Demina,⁷ L. Demortier,³¹ M. Deninno,² P. F. Derwent,⁷ T. Devlin,³² J. R. Dittmann,⁶ S. Donati,²⁷ J. Done,³⁴ T. Dorigo,²⁵ N. Eddy,²⁰ K. Einsweiler,¹⁸ J. E. Elias,⁷ R. Ely,¹⁸ E. Engles,⁷ Jr.,²⁸ W. Erdmann,⁷ D. Errede,¹³ S. Errede,¹³ Q. Fan,³⁰ R. G. Feild,⁴¹ Z. Feng,¹⁵ C. Ferretti,²⁷ I. Fiori,² B. Flaugher,⁷ G. W. Foster,⁷ M. Franklin,¹¹ J. Freeman,⁷ J. Friedman,¹⁹ H. Frisch,⁵ Y. Fukui,¹⁷ S. Gadomski,¹⁴ S. Galeotti,²⁷ M. Gallinaro,²⁶ O. Ganel,³⁵ M. Garcia-Sciveres,¹⁸ A. F. Garfinkel,²⁹ C. Gay,⁴¹ S. Geer,⁷ D. W. Gerdes,¹⁵ P. Giannetti,²⁷ N. Giokaris,³¹ P. Giromini,⁹ G. Giusti,²⁷ M. Gold,²² A. Gordon,¹¹ A. T. Goshaw,⁶ Y. Gotra,²⁵ K. Goulianos,³¹ H. Grassmann,³⁶ L. Groer,³² C. Grossi-Pilcher,⁵ G. Guillian,²⁰ J. Guimaraes da Costa,¹⁵ R. S. Guo,³³ C. Haber,¹⁸ E. Hafen,¹⁹ S. R. Hahn,⁷ R. Hamilton,¹¹ T. Handa,¹² R. Handler,⁴⁰ F. Happacher,⁹ K. Hara,³⁷ A. D. Hardman,²⁹ R. M. Harris,⁷ F. Hartmann,¹⁶ J. Hauser,⁴ E. Hayashi,³⁷ J. Heinrich,²⁶ W. Hao,³⁵ B. Hinrichsen,¹⁴ K. D. Hoffman,²⁹ M. Hohlmann,⁵ C. Holck,²⁶ R. Hollebeek,²⁶ L. Holloway,¹³ Z. Huang,²⁰ B. T. Huffman,²⁸ R. Hughes,²³ J. Huston,²¹ J. Huth,¹¹ H. Ikeda,³⁷ M. Incagli,²⁷ J. Incandela,⁷ G. Introzzi,²⁷ J. Iwai,³⁹ Y. Iwata,¹² E. James,²⁰ H. Jensen,⁷ U. Joshi,⁷ R. W. Kadel,¹⁸ E. Kajfasz,²⁵ H. Kambara,¹⁰ T. Kamon,³⁴ T. Kaneko,³⁷ K. Karr,³⁸ H. Kasha,⁴¹ Y. Kato,²⁴ T. A. Keaffaber,²⁹ K. Kelley,¹⁹ R. D. Kennedy,⁷ R. Kephart,⁷ D. Kestenbaum,¹¹ D. Khazins,⁶ T. Kikuchi,³⁷ B. J. Kim,²⁷ H. S. Kim,¹⁴ S. H. Kim,³⁷ Y. K. Kim,¹⁸ L. Kirsch,³ S. Klimentko,⁸ D. Knoblauch,¹⁶ P. Koehn,²³ A. Konigeter,¹⁶ K. Kondo,³⁷ J. Konigsberg,⁸ K. Kordas,¹⁴ A. Korytov,⁸ E. Kovacs,¹ W. Kowald,⁶ J. Kroll,²⁶ M. Kruse,³⁰ S. E. Kuhlmann,¹ E. Kuns,³² K. Kurino,¹² T. Kuwabara,³⁷ A. T. Laasanen,²⁹ I. Nakano,¹² S. Lami,²⁷ S. Lammel,⁷ J. I. Lamoureux,³ M. Lancaster,¹⁸ M. Lanzoni,²⁷ G. Latino,²⁷ T. LeCompte,¹ S. Leone,²⁷ J. D. Lewis,⁷ P. Limon,⁷ M. Lindgren,⁴ T. M. Liss,¹³ J. B. Liu,³⁰ Y. C. Liu,³³ N. Lockyer,²⁶ O. Long,²⁶ C. Loomis,³² M. Loreti,²⁵ D. Lucchesi,²⁷ P. Lukens,⁷ S. Lusin,⁴⁰ J. Lys,¹⁸ K. Maeshima,⁷ P. Maksimovic,¹⁹ M. Mangano,²⁷ M. Mariotti,²⁵ J. P. Marriner,⁷ A. Martin,⁴¹ J. A. J. Matthews,²² P. Mazzanti,² P. McIntyre,³⁴ P. Melese,³¹ M. Menguzzato,²⁵ A. Menzione,²⁷ E. Meschi,²⁷ S. Metzler,²⁶ C. Miao,²⁰ T. Miao,⁷ G. Michail,¹¹ R. Miller,²¹ H. Minato,³⁷ S. Miscetti,⁹ M. Mishina,¹⁷ S. Miyashita,³⁷ N. Moggi,²⁷ E. Moore,²² Y. Morita,¹⁷ A. Mukherjee,⁷ T. Muller,¹⁶ P. Murat,²⁷ S. Murgia,²¹ H. Nakada,³⁷ I. Nakano,¹² C. Nelson,⁷ D. Neuberger,¹⁶ C. Newman-Holmes,⁷ C.-Y. P. Ngan,¹⁹ L. Nodulman,¹ A. Nomerotski,⁸ S. H. Oh,⁶ T. Ohmoto,¹² T. Ohsugi,¹² R. Oishi,³⁷ M. Okabe,³⁷ T. Okusawa,²⁴ J. Olsen,⁴⁰ C. Pagliarone,²⁷ R. Paoletti,²⁷ V. Papadimitriou,³⁵ S. P. Pappas,⁴¹ N. Parashar,²⁷ A. Parri,⁹ J. Patrick,⁷ G. Pauletta,³⁶ M. Paulini,¹⁸ A. Perazzo,²⁷ L. Pescara,²⁵ M. D. Peters,¹⁸ T. J. Phillips,⁶ G. Piacentino,²⁷ M. Pillai,³⁰ K. T. Pitts,⁷ R. Plunkett,⁷ A. Pompos,²⁹ L. Pondrom,⁴⁰ J. Proudfoot,¹ F. Ptoshos,¹¹ G. Punzi,²⁷ K. Ragan,¹⁴ D. Reher,¹⁸ M. Reischl,¹⁶ A. Ribon,²⁵ F. Rimondi,² L. Ristori,²⁷ W. J. Robertson,⁶ T. Rodrigo,²⁷ S. Rolli,³⁸ L. Rosenson,¹⁹ R. Roser,¹³ T. Saab,¹⁴ W. K. Sakamoto,³⁰ D. Saltzberg,⁴ A. Sansoni,⁹ L. Santi,³⁶ H. Sato,³⁷ P. Schlabach,⁷ E. E. Schmidt,⁷ M. P. Schmidt,⁴¹ A. Scott,⁴ A. Scribano,²⁷ S. Segler,⁷ S. Seidel,²² Y. Seiya,³⁷ F. Semeria,² T. Shah,¹⁹ M. D. Shapiro,¹⁸ N. M. Shaw,²⁹ P. F. Shepard,²⁸ T. Shibayama,³⁷ M. Shimojima,³⁷ M. Shochet,⁵ J. Siegrist,¹⁸ A. Sill,³⁵ P. Sinervo,¹⁴ P. Singh,¹³ K. Sliwa,³⁸ C. Smith,¹⁵ F. D. Snider,¹⁵ J. Spalding,⁷ T. Speer,¹⁰ P. Sphicas,¹⁹ F. Spinella,²⁷ M. Spiropulu,¹¹ L. Spiegel,⁷ L. Stanco,²⁵ J. Steele,⁴⁰ A. Stefanini,²⁷ R. Ströhmer,^{7,*} J. Strologas,¹³ F. Strumia,¹⁰ D. Stuart,⁷ K. Sumorok,¹⁹ J. Suzuki,³⁷ T. Suzuki,³⁷ T. Takahashi,²⁴ T. Takano,²⁴ R. Takashima,¹² K. Takikawa,³⁷ M. Tanaka,³⁷ B. Tannenbaum,²² F. Tartarelli,²⁷ W. Taylor,¹⁴ M. Tecchio,²⁰ P. K. Teng,³³ Y. Teramoto,²⁴ K. Terashi,³⁷ S. Tether,¹⁹ D. Theriot,⁷ T. L. Thomas,²² R. Thurman-Keup,¹ M. Timko,³⁸ P. Tipton,³⁰ A. Titov,³¹ S. Tkaczuk,⁷ D. Toback,⁵ K. Tollefson,¹⁹ A. Tollestrup,⁷ H. Toyoda,²⁴ W. Trischuk,¹⁴ J. F. de Troconiz,¹¹ S. Truitt,²⁰ J. Tseng,¹⁹ N. Turini,²⁷ T. Uchida,³⁷ F. Ukegawa,²⁶ J. Valls,³² S. C. van den Brink,²⁸ S. Vejcik III,²⁰ G. Velev,²⁷ R. Vidal,⁷ R. Vilar,^{7,*} D. Vucinic,¹⁹ R. G. Wagner,¹ R. L. Wagner,⁷ J. Wahl,⁵ N. B. Wallace,²⁷ A. M. Walsh,³² C. Wang,⁶ C. H. Wang,³³ M. J. Wang,³³ A. Warburton,¹⁴ T. Watanabe,³⁷ T. Watts,³² R. Webb,³⁴ C. Wei,⁶ H. Wenzel,¹⁶ W. C. Wester III,⁷ A. B. Wicklund,¹ E. Wicklund,⁷ R. Wilkinson,²⁶ H. H. Williams,²⁶ P. Wilson,⁵ B. L. Winer,²³ D. Winn,²⁰ D. Wolinski,²⁰ J. Wolinski,²¹ S. Worm,²² X. Wu,¹⁰ J. Wyss,²⁷ A. Yagil,⁷ W. Yao,¹⁸ K. Yasuoka,³⁷ G. P. Yeh,⁷ P. Yeh,³³ J. Yoh,⁷ C. Yosef,²¹ T. Yoshida,²⁴ I. Yu,⁷ A. Zanetti,³⁶ F. Zetti,²⁷ and S. Zucchelli²

(CDF Collaboration)

- ¹Argonne National Laboratory, Argonne, Illinois 60439
²Istituto Nazionale di Fisica Nucleare, University of Bologna, I-40127 Bologna, Italy
³Brandeis University, Waltham, Massachusetts 02254
⁴University of California at Los Angeles, Los Angeles, California 90024
⁵University of Chicago, Chicago, Illinois 60637
⁶Duke University, Durham, North Carolina 27708
⁷Fermi National Accelerator Laboratory, Batavia, Illinois 60510
⁸University of Florida, Gainesville, Florida 32611
⁹Laboratori Nazionali di Frascati, Istituto Nazionale di Fisica Nucleare, I-00044 Frascati, Italy
¹⁰University of Geneva, CH-1211 Geneva 4, Switzerland
¹¹Harvard University, Cambridge, Massachusetts 02138
¹²Hiroshima University, Higashi-Hiroshima 724, Japan
¹³University of Illinois, Urbana, Illinois 61801
¹⁴Institute of Particle Physics, McGill University, Montreal, Canada H3A 2T8
and University of Toronto, Toronto, Canada M5S 1A7
¹⁵The Johns Hopkins University, Baltimore, Maryland 21218
¹⁶Institut für Experimentelle Kernphysik, Universität Karlsruhe, 76128 Karlsruhe, Germany
¹⁷National Laboratory for High Energy Physics (KEK), Tsukuba, Ibaraki 305, Japan
¹⁸Ernest Orlando Lawrence Berkeley National Laboratory, Berkeley, California 94720
¹⁹Massachusetts Institute of Technology, Cambridge, Massachusetts 02139
²⁰University of Michigan, Ann Arbor, Michigan 48109
²¹Michigan State University, East Lansing, Michigan 48824
²²University of New Mexico, Albuquerque, New Mexico 87131
²³The Ohio State University, Columbus, Ohio 43210
²⁴Osaka City University, Osaka 588, Japan
²⁵Università di Padova, Istituto Nazionale di Fisica Nucleare, Sezione di Padova, I-35131 Padova, Italy
²⁶University of Pennsylvania, Philadelphia, Pennsylvania 19104
²⁷Istituto Nazionale de Fisica Nucleare, University and Scuola Normale Superiore of Pisa, I-56100 Pisa, Italy
²⁸University of Pittsburgh, Pittsburgh, Pennsylvania 15260
²⁹Purdue University, West Lafayette, Indiana 47907
³⁰University of Rochester, Rochester, New York 14627
³¹Rockefeller University, New York, New York, 10021
³²Rutgers University, Piscataway, New Jersey 08855
³³Academia Sinica, Taipei, Taiwan 11530, Republic of China
³⁴Texas A&M University, College Station, Texas 77843
³⁵Texas Tech University, Lubbock, Texas 79409
³⁶Istituto Nazionale di Fisica Nucleare, University of Trieste/Udine, Italy
³⁷University of Tsukuba, Tsukuba, Ibaraki 315, Japan
³⁸Tufts University, Medford, Massachusetts 02155
³⁹Waseda University, Tokyo 169, Japan
⁴⁰University of Wisconsin, Madison, Wisconsin 53706
⁴¹Yale University, New Haven, Connecticut 06520

(Received 17 March 1998; published 8 July 1998)

We have searched for the rare decay $W^\pm \rightarrow \pi^\pm + \gamma$ in 83 pb^{-1} of data taken in proton-antiproton collisions at $\sqrt{s} = 1.8 \text{ TeV}$ with the Collider Detector at Fermilab. We find three events in the signal region and estimate the background to be 5.2 ± 1.5 events. We set a 95% confidence level upper limit of 7×10^{-4} on the ratio of partial widths, $\Gamma(W^\pm \rightarrow \pi^\pm + \gamma)/\Gamma(W^\pm \rightarrow e^\pm + \nu)$.

[S0556-2821(98)50115-4]

PACS number(s): 13.38.Be, 13.40.Hq, 13.85.Qk

Rare decays of the W boson provide precision tests of the standard model of electroweak interactions. The ratio of the partial widths of the decays $W^\pm \rightarrow \pi^\pm + \gamma$ to $W^\pm \rightarrow e^\pm + \nu$ is predicted [1] to be $\Gamma(W^\pm \rightarrow \pi^\pm + \gamma)/\Gamma(W^\pm \rightarrow e^\pm + \nu) \simeq 3 \times 10^{-8}$. Observation of this decay in excess of the theoreti-

cal prediction could be an indicator of physics beyond the standard model. Data taken during 1992–1993 (run Ia) with the Collider Detector at Fermilab (CDF) have allowed us to set an upper limit [2] on this ratio of 2.0×10^{-3} at the 95% confidence level (C.L.) on the basis of 16 pb^{-1} of integrated luminosity. In this paper we extend the analysis to a data sample five times larger.

The CDF detector has been described elsewhere [3]. We

*Visitor.

use a coordinate system where ϕ is the azimuthal angle around the beam line and θ is the polar angle with respect to the z (proton beam) direction. Pseudorapidity η is defined by $\eta = -\ln(\tan(\theta/2))$; p_T ($= P \sin \theta$) and E_T ($= E \sin \theta$) are the momentum and energy flow measured transverse to the beam line, respectively.

Data for this analysis were collected during 1994–1995 (run Ib) with proton-antiproton collisions at a center of mass energy of 1.8 TeV. The data sample consists of a total of 2.45 million photon candidate events selected with a three level trigger. The first level trigger required total energy greater than 8 GeV in a contiguous pair of central ($|\eta| < 1.1$) electromagnetic (EM) calorimeter towers. The second level trigger imposed a photon energy threshold of 23 GeV and required that the photon be isolated. The isolation criteria required that less than 4 GeV of additional transverse energy be found in a 6×3 grid of calorimeter towers (corresponding approximately to a cone in $\eta-\phi$ space of $\Delta R = \sqrt{\Delta\eta^2 + \Delta\phi^2} \sim 0.4$) centered on the photon direction. Photon candidates which passed the third level trigger were required to be in the fiducial region of the calorimeter.

The trigger did not reject photon candidates with associated charged tracks; therefore, isolated electrons could satisfy the photon trigger requirements. The threshold dependence of the photon trigger has been measured by comparison with photons from a trigger with a nominal energy threshold of 10 GeV and electrons from $W^\pm \rightarrow e^\pm + \nu$ decay collected with a different trigger. The photon trigger efficiency, when convoluted with the expected p_T spectrum of photons from $W^\pm \rightarrow \pi^\pm + \gamma$, is estimated to be $0.844 \pm 0.025(\text{stat.}) \pm 0.020(\text{sys.})$, including the hardware efficiency, threshold dependence, and isolation cut.

All events were passed through two analysis paths: one designed to select photons and a second designed to select jets [4] with isolated, high p_T tracks. Events from each path were used to produce efficiency and background estimates. Information for events surviving both selections was assembled, and overall event topology cuts were applied to yield candidate events satisfying the $W^\pm \rightarrow \pi^\pm + \gamma$ decay hypothesis. In the discussion that follows we first summarize the data reduction of the photon and then the pion analysis paths. We then compare estimates of the detection efficiency made with Monte Carlo simulations (PAPAGENO [5]) to estimates taken directly from the data. We use the ratio of these to correct the predictions of the Monte Carlo simulation. Finally, we use the data sample to estimate the background and compute the 95% C.L. limit on the cross section times branching ratio ($\sigma \cdot B$) for the decay.

In the photon analysis, we first correct the photon energies in order to optimize the energy resolution using corrections derived from the electron trigger samples [6]. We next require that photon candidates have no reconstructed track pointing at the calorimeter cells containing the EM shower. All events considered further must have passed the photon trigger and have an event vertex (z_{vertex}) within ± 60 cm of the nominal interaction point. The direction of the photon is computed from the event vertex and the location of the shower as measured in proportional chambers six radiation lengths deep in the calorimeter. We also require the trans-

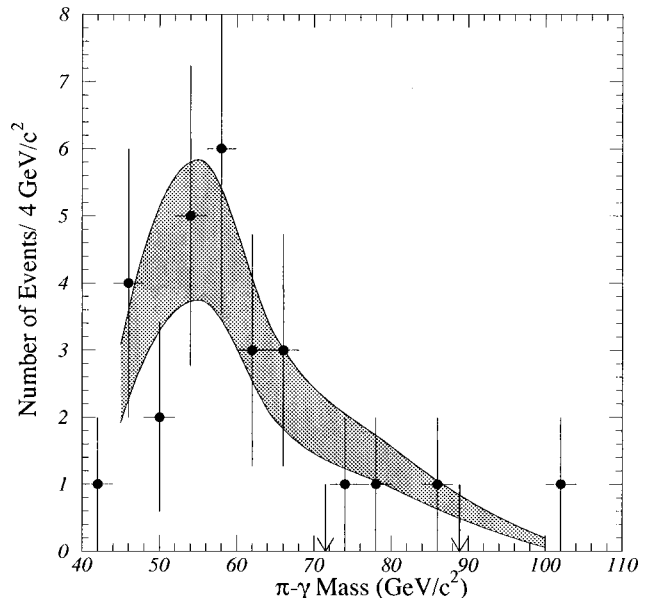


FIG. 1. Distribution of the $\pi\gamma$ mass for the 28 events of the signal sample in bins of $4 \text{ GeV}/c^2$. The shaded band shows the one sigma uncertainty in the background expectation value. There are three events in the W mass region (between the two arrows), with an estimated background of 5.2 ± 1.5 events.

verse shower shape, as measured by the shower profile proportional chambers and the lateral sharing of energy between neighboring calorimeter towers, to be consistent with a single EM shower as measured in test beam data. In the offline analysis we tighten the isolation cut to require less than 4 GeV of E_T in a cone of $\Delta R < 0.7$ around the photon direction.

In the isolated pion analysis we search the full data sample for jets with $E_T > 15$ GeV that are consistent with a single charge pion. We require a central jet ($|\eta| < 1.1$), with exactly one tract with $p_T > 15 \text{ GeV}/c$, and no other tracks with p_T greater than $1 \text{ GeV}/c$ in a cone of radius $\Delta R = 0.7$ around the high p_T track. The high p_T track must pass within ± 5 cm of the event vertex in the z coordinate. The track is constrained to come from the beam line. To verify that the energy in the calorimeter is consistent with that coming from a single track, we require the charged fraction (CHFR), defined as the ratio of the track p_T to the total calorimeter jet E_T , to be greater than 1.0. Of the 2.45 M events, 28.1 K survive the single track jet cuts. This sample is dominated by electrons, with the charged particle matched to a photon trigger candidate. The additional requirement that the EM fraction (EMFR) of the jet energy be less than 80% of the total calorimeter energy removes all but 886 events.

Finally, to select $W^\pm \rightarrow \pi^\pm + \gamma$ candidates, we pick events from the data sample with one photon candidate, one jet consistent with a single charged pion, the track and the photon separated by at least $\Delta\phi > 1.5$ radians, and no other jets with $E_T > 15$ GeV. After these cuts 28 events remain (Fig. 1). Three events are within $\pm 8.7 \text{ GeV}/c^2$ (three times our mass resolution) of the W mass. We refer to these 28 events as the “signal sample.”

Where possible, we have checked the event selection ef-

TABLE I. Efficiencies for various cuts compared to the values obtained from the Monte Carlo simulation. The uncertainties quoted in the $W^\pm \rightarrow e^\pm + \nu$ efficiency column are statistical only. The statistical uncertainties on the Monte Carlo simulation are always less than or equal to the statistical uncertainty on the result from $W^\pm \rightarrow e^\pm + \nu$ events, and are included in the uncertainty on the ratio, which is quoted first with statistical, then systematic uncertainties.

Requirement	Monte Carlo efficiency	Run Ib $W^\pm \rightarrow e^\pm + \nu$ efficiency	Ratio
EMFR<0.8	0.960	0.968 ± 0.003	$1.008 \pm 0.003 \pm 0.011$
CHFR>1.0	0.773	0.760 ± 0.007	$0.983 \pm 0.010 \pm 0.060$
Track isolation	0.710	0.718 ± 0.007	$1.011 \pm 0.007 \pm 0.020$
Shower shape	0.970	0.976 ± 0.003	$1.006 \pm 0.004 \pm 0.017$
$E_T < 4.0$ GeV ($\Delta R < 0.7$)	0.968	0.913 ± 0.004	$0.943 \pm 0.004 \pm 0.030$
$ z_{\text{vertex}} < 60$ cm	0.973	0.956 ± 0.002	$0.982 \pm 0.003 \pm 0.011$
Total Monte Carlo correction factor			$0.933 \pm 0.014 \pm 0.073$

ficiency directly from the data sample, using $W^\pm \rightarrow e^\pm + \nu$ events collected from the photon trigger. We embed a simulated pion with the momentum of the neutrino in these events to check our single track jet analysis, and use the electron from the $W^\pm \rightarrow e^\pm + \nu$ decay to test our photon cuts.

To find events consistent with the $W^\pm \rightarrow e^\pm + \nu$ decay we select events from the single track jet data sample by requiring exactly one jet with E_T greater than 15 GeV containing at least 15 GeV of energy in the electromagnetic calorimeter. From the imbalance in transverse energy measured in each event (missing E_T , or \cancel{E}_T) we try to reconstruct the possible directions of a neutrino in $W^\pm \rightarrow e^\pm + \nu$ decay. Given the W mass, the electron momentum, and the two components of the \cancel{E}_T , there are two possible results for the neutrino direction. If the results yield physical solutions for the ν momentum, we choose those events in which the ν longitudinal momentum is consistent with $|\eta_\nu| < 1.1$. If both solutions satisfy this requirement, we choose randomly between them. In this way at most one solution per event is used and events with nonphysical solutions are discarded.

We assign the neutrino momentum to a simulated pion, which we embed in these events to calculate the efficiency of the jet EM fraction and charged fraction cuts. This technique explicitly includes the effects of the underlying event in the cut. The efficiencies for the EMFR and CHFR cuts determined in this way are 0.968 ± 0.003 (stat.), and 0.760 ± 0.007 (stat.), respectively, (Table I). To estimate the systematic uncertainty of our procedure, we add the change in the average value of the EMFR and CHFR (between the Monte Carlo simulation and the simulation based on the $W^\pm \rightarrow e^\pm + \nu$ data) to the cut, and redo the analysis. This results in the EMFR cut being changed from 0.80 to 0.83, and the CHFR cut being changed from 1.00 to 1.03. We find that the efficiency of the EMFR cut changes by only 0.011, but because the cut on CHFR is made near the maximum of the CHFR distribution, there is a change of 0.045 in the CHFR efficiency.

The efficiency of the track-isolation cut on the pion candidate (no additional track with $p_T > 1$ GeV/c around the pion candidate) is determined by imposing the same cut

around the neutrino direction. The efficiency is measured to be 0.718 ± 0.007 (stat.) ± 0.018 (sys.).

From the electron candidate in these $W^\pm \rightarrow e^\pm + \nu$ events, we estimate the detection efficiency for cuts on the photon transverse shower shape to be 0.976 ± 0.003 (stat.). The Monte Carlo simulation reproduces the observed photon transverse shower profile distributions well. We assign a systematic error of 0.017 to account for electron bremsstrahlung and observed differences between the Monte Carlo simulation and the data.

The efficiency of the 4 GeV photon isolation cut is measured by looking at the efficiency of the same cut in a cone of $\Delta R = 0.7$ around the neutrino direction. The efficiency measured in this way is 0.913 ± 0.004 (stat.). To estimate the systematic uncertainty on this number we compare the average isolation energy in the neutrino direction and the electron direction. The difference in mean isolation energy in the two directions is 0.13 GeV. We then recalculate the efficiency of the isolation cut, changing the cut value from 4.00 to 4.13 GeV. From this analysis we assign a systematic uncertainty of 0.03 to the measurement of the efficiency on the isolation. The efficiency of the z -vertex cut has been measured to be 0.956 ± 0.002 (stat.) ± 0.011 (sys.).

The comparison between the measured efficiencies and the Monte Carlo simulation is summarized in Table II. Based on these studies, we apply a correction of 0.933 ± 0.014 (stat.) ± 0.073 (sys.) to the overall acceptance determined from the Monte Carlo simulation.

TABLE II. Contributions to the overall efficiency and acceptance calculation and their uncertainties.

Contribution	Value	Statistical uncertainty	Systematic uncertainty
Monte Carlo efficiency	0.0476	± 0.0002	± 0.0033
Correction factor	0.933	± 0.014	± 0.073
Trigger efficiency	0.844	± 0.025	± 0.020
Luminosity	1.000	-	± 0.080
Net efficiency	0.0375	± 0.0011	± 0.0050

We expect the final data sample to be dominated by background events from QCD processes. The predominant background is expected to be a direct photon production, in which a photon candidate is identified in the detector, and an additional parton fragments into a single charged particle. To estimate this background and avoid trigger biases, we use a subset of events which satisfy the photon requirements and general event topology cuts, but fail the single-track jet cuts. We combine the momentum vectors of all the charged tracks (at least three are required) with $p_T > 1$ GeV/c in the jet opposite the photon to form a single charged “pseudotrack.” This jet is then required to meet all of our standard jet criteria, except for the number of charged tracks/jet. In addition, we require the total charge of all tracks making up the pseudotrack to be ± 1 . We have combined the charged track momenta three different ways to form the pseudotrack, and all give similar results [7]. As reported in Ref. [2], we have found that within a mass bin of width $\Delta M = 10\text{--}20$ GeV/c 2 , the number of events is a linear function of the number of tracks used to create the pseudotrack. We have taken our pseudotrack background data sample (1477 events) and divided it into five mass bins (40–50 GeV/c 2 , 50–60 GeV/c 2 , 60–70 GeV/c 2 , 70–90 GeV/c 2 , and 90–110 GeV/c 2), and within each mass bin we fit with a straight line the fraction of events versus the number of tracks used to create the pseudotrack. This line is then extrapolated to 1 track/jet. We then take the points obtained from these extrapolations (the W mass region is excluded), normalize the area to 25 events, and compute the number of events in the W mass window. We find 5.2 ± 1.5 background events. A simpler background estimate where the shape of the pseudotrack background is normalized to the

number of events in the signal sample using a single constant gives an identical result.

Figure 1 shows the 28 signal events along with this background estimate. The uncorrected Monte Carlo efficiency \times acceptance ($\epsilon \times A$) is $0.0476 \pm 0.0002(\text{stat.}) \pm 0.0033(\text{sys.})$. The overall efficiency reflects mainly the calorimeter fiducial cuts, the η cuts ($|\eta| < 1.1$) on the photon and pion directions, together with the isolation cut on the single track jet. From the above studies, we find the corrected net $\epsilon \times A$ for the decay $W^\pm \rightarrow \pi^\pm + \gamma$ to be $0.038 \pm 0.001(\text{stat.}) \pm 0.005(\text{sys.})$, including the trigger efficiency, uncertainties in luminosity, all analysis cuts, and a 7% uncertainty because of structure function variation [8]. Using Poisson statistics [9], including the background estimate, its uncertainty, and the variation in the acceptance, we compute a limit of 5.2 events at the 95% C.L. limit. Defining $\sigma \cdot B = N_{\text{evt}} / (A \times \epsilon \times \mathcal{L})$, where N_{evt} is the number of events and \mathcal{L} is the integrated luminosity (83 pb $^{-1}$), we conclude that $\sigma \cdot B(W^\pm \rightarrow \pi^\pm + \gamma) \leq 1.7$ pb at the 95% C.L. Dividing this result by our value of $\sigma \cdot B(W^\pm \rightarrow e^\pm + \nu) = 2.49 \pm 0.12$ nb [10], we find $\Gamma(W^\pm \rightarrow \pi^\pm + \gamma) / \Gamma(W^\pm \rightarrow e^\pm + \nu) \leq 7 \times 10^{-4}$ at the 95% C.L. This limit is a factor of three times better than our previous result [2].

We wish to thank the Accelerator Division of Fermi National Accelerator Laboratory, and the technical staffs of the participating institutions for their vital contributions. This work was supported by the U.S. Department of Energy and National Science Foundation, the Italian Istituto Nazionale di Fisica Nucleare, the Ministry of Education, Science and Culture of Japan, the Natural Sciences and Engineering Research Council of Canada, the National Science Council of the Republic of China, and the A. P. Sloan Foundation.

-
- [1] L. Arnellos *et al.*, Nucl. Phys. **B196**, 378 (1982).
 - [2] CDF Collaboration, F. Abe *et al.*, Phys. Rev. Lett. **76**, 2852 (1996).
 - [3] CDF Collaboration, F. Abe *et al.*, Nucl. Instrum. Methods Phys. Res. A **271**, 387 (1988).
 - [4] CDF Collaboration, F. Abe *et al.*, Phys. Rev. D **45**, 1448 (1992).
 - [5] I. Hinchliffe, in *Proceedings of the Workshop on Physics at Current Accelerators and Supercolliders*, Argonne, Illinois, 1993, edited by J. L. Hewett, A. R. White, and D. Zeppenfeld (ANL Report No. 93-92, Argonne, 1993), pp. 679–686.
 - [6] CDF Collaboration, F. Abe *et al.*, Phys. Rev. D **52**, 4784 (1995).
 - [7] We investigated three methods of combining momenta: (1)

- Add all 4-vectors together. In this case the pseudotrack acquires a rest mass that is in general not equal to a pion mass.
- (2) Add the three momenta and give the resulting pseudotrack an energy derived from the total 3-momentum plus the pion rest mass. This technique removes energy from the jet.
- (3) Use the pseudotrack energy, and rescale the total 3-momentum, without changing its direction, so the pseudotrack has the rest mass of a pion.
- [8] CDF Collaboration, F. Abe *et al.*, Phys. Rev. Lett. **69**, 2160 (1992).
- [9] Particle Data Group, R. M. Barnett *et al.*, Phys. Rev. D **54**, 1 (1996), p. 166.
- [10] CDF Collaboration, F. Abe *et al.*, Phys. Rev. Lett. **76**, 3070 (1996).